

Precise Measurement of the Top Quark Mass in the Dilepton Channel at D0

V. M. Abazov,³⁵ B. Abbott,⁷³ B. S. Acharya,²⁹ M. Adams,⁴⁹ T. Adams,⁴⁷ G. D. Alexeev,³⁵ G. Alkhazov,³⁹ A. Alton,^{61,*} G. Alverson,⁶⁰ G. A. Alves,² L. S. Ancu,³⁴ M. Aoki,⁴⁸ M. Arov,⁵⁸ A. Askew,⁴⁷ B. Åsman,⁴¹ O. Atramentov,⁶⁵ C. Avila,⁸ J. BackusMayes,⁸⁰ F. Badaud,¹³ L. Bagby,⁴⁸ B. Baldin,⁴⁸ D. V. Bandurin,⁴⁷ S. Banerjee,²⁹ E. Barberis,⁶⁰ P. Baringer,⁵⁶ J. Barreto,³ J. F. Bartlett,⁴⁸ U. Bassler,¹⁸ V. Bazterra,⁴⁹ S. Beale,⁶ A. Bean,⁵⁶ M. Begalli,³ M. Begel,⁷¹ C. Belanger-Champagne,⁴¹ L. Bellantoni,⁴⁸ S. B. Beri,²⁷ G. Bernardi,¹⁷ R. Bernhard,²² I. Bertram,⁴² M. Besançon,¹⁸ R. Beuselinck,⁴³ V. A. Bezzubov,³⁸ P. C. Bhat,⁴⁸ V. Bhatnagar,²⁷ G. Blazey,⁵⁰ S. Blessing,⁴⁷ K. Bloom,⁶⁴ A. Boehnlein,⁴⁸ D. Boline,⁷⁰ E. E. Boos,³⁷ G. Borissov,⁴² T. Bose,⁵⁹ A. Brandt,⁷⁶ O. Brandt,²³ R. Brock,⁶² G. Brooijmans,⁶⁸ A. Bross,⁴⁸ D. Brown,¹⁷ J. Brown,¹⁷ X. B. Bu,⁴⁸ M. Buehler,⁷⁹ V. Buescher,²⁴ V. Bunichev,³⁷ S. Burdin,^{42,†} T. H. Burnett,⁸⁰ C. P. Buszello,⁴¹ B. Calpas,¹⁵ E. Camacho-Pérez,³² M. A. Carrasco-Lizarraga,⁵⁶ B. C. K. Casey,⁴⁸ H. Castilla-Valdez,³² S. Chakrabarti,⁷⁰ D. Chakraborty,⁵⁰ K. M. Chan,⁵⁴ A. Chandra,⁷⁸ G. Chen,⁵⁶ S. Chevalier-Théry,¹⁸ D. K. Cho,⁷⁵ S. W. Cho,³¹ S. Choi,³¹ B. Choudhary,²⁸ S. Cihangir,⁴⁸ D. Claes,⁶⁴ J. Clutter,⁵⁶ M. Cooke,⁴⁸ W. E. Cooper,⁴⁸ M. Corcoran,⁷⁸ F. Couderc,¹⁸ M.-C. Cousinou,¹⁵ A. Croc,¹⁸ D. Cutts,⁷⁵ A. Das,⁴⁵ G. Davies,⁴³ K. De,⁷⁶ S. J. de Jong,³⁴ E. De La Cruz-Burelo,³² F. Déliot,¹⁸ M. Demarteau,⁴⁸ R. Demina,⁶⁹ D. Denisov,⁴⁸ S. P. Denisov,³⁸ S. Desai,⁴⁸ C. Deterre,¹⁸ K. DeVaughan,⁶⁴ H. T. Diehl,⁴⁸ M. Diesburg,⁴⁸ A. Dominguez,⁶⁴ T. Dorland,⁸⁰ A. Dubey,²⁸ L. V. Dudko,³⁷ D. Duggan,⁶⁵ A. Duperrin,¹⁵ S. Dutt,²⁷ A. Dyshkant,⁵⁰ M. Eads,⁶⁴ D. Edmunds,⁶² J. Ellison,⁴⁶ V. D. Elvira,⁴⁸ Y. Enari,¹⁷ H. Evans,⁵² A. Evdokimov,⁷¹ V. N. Evdokimov,³⁸ G. Facini,⁶⁰ T. Ferbel,⁶⁹ F. Fiedler,²⁴ F. Filthaut,³⁴ W. Fisher,⁶² H. E. Fisk,⁴⁸ M. Fortner,⁵⁰ H. Fox,⁴² S. Fuess,⁴⁸ A. Garcia-Bellido,⁶⁹ V. Gavrilov,³⁶ P. Gay,¹³ W. Geng,^{15,62} D. Gerbaudo,⁶⁶ C. E. Gerber,⁴⁹ Y. Gershtein,⁶⁵ G. Ginther,^{48,69} G. Golovanov,³⁵ A. Goussiou,⁸⁰ P. D. Grannis,⁷⁰ S. Greder,¹⁹ H. Greenlee,⁴⁸ Z. D. Greenwood,⁵⁸ E. M. Gregores,⁴ G. Grenier,²⁰ Ph. Gris,¹³ J.-F. Grivaz,¹⁶ A. Grohsjean,¹⁸ S. Grünendahl,⁴⁸ M. W. Grünewald,³⁰ T. Guillemin,¹⁶ F. Guo,⁷⁰ G. Gutierrez,⁴⁸ P. Gutierrez,⁷³ A. Haas,^{68,‡} S. Hagopian,⁴⁷ J. Haley,⁶⁰ L. Han,⁷ K. Harder,⁴⁴ A. Harel,⁶⁹ J. M. Hauptman,⁵⁵ J. Hays,⁴³ T. Head,⁴⁴ T. Hebbeker,²¹ D. Hedin,⁵⁰ H. Hegab,⁷⁴ A. P. Heinson,⁴⁶ U. Heintz,⁷⁵ C. Hensel,²³ I. Heredia-De La Cruz,³² K. Herner,⁶¹ G. Hesketh,^{44,§} M. D. Hildreth,⁵⁴ R. Hirosky,⁷⁹ T. Hoang,⁴⁷ J. D. Hobbs,⁷⁰ B. Hoeneisen,¹² M. Hohlfeld,²⁴ Z. Hubacek,^{10,18} N. Huske,¹⁷ V. Hynek,¹⁰ I. Iashvili,⁶⁷ R. Illingworth,⁴⁸ A. S. Ito,⁴⁸ S. Jabeen,⁷⁵ M. Jaffré,¹⁶ D. Jamin,¹⁵ A. Jayasinghe,⁷³ R. Jesik,⁴³ K. Johns,⁴⁵ M. Johnson,⁴⁸ D. Johnston,⁶⁴ A. Jonckheere,⁴⁸ P. Jonsson,⁴³ J. Joshi,²⁷ A. W. Jung,⁴⁸ A. Juste,⁴⁰ K. Kaadze,⁵⁷ E. Kajfasz,¹⁵ D. Karmanov,³⁷ P. A. Kasper,⁴⁸ I. Katsanos,⁶⁴ R. Kehoe,⁷⁷ S. Kermiche,¹⁵ N. Khalatyan,⁴⁸ A. Khanov,⁷⁴ A. Kharchilava,⁶⁷ Y. N. Kharzheev,³⁵ D. Khatidze,⁷⁵ M. H. Kirby,⁵¹ J. M. Kohli,²⁷ A. V. Kozelov,³⁸ J. Kraus,⁶² S. Kulikov,³⁸ A. Kumar,⁶⁷ A. Kupco,¹¹ T. Kurča,²⁰ V. A. Kuzmin,³⁷ J. Kvita,⁹ S. Lammers,⁵² G. Landsberg,⁷⁵ P. Lebrun,²⁰ H. S. Lee,³¹ S. W. Lee,⁵⁵ W. M. Lee,⁴⁸ J. Lellouch,¹⁷ L. Li,⁴⁶ Q. Z. Li,⁴⁸ S. M. Lietti,⁵ J. K. Lim,³¹ D. Lincoln,⁴⁸ J. Linnemann,⁶² V. V. Lipaev,³⁸ R. Lipton,⁴⁸ Y. Liu,⁷ Z. Liu,⁶ A. Lobodenko,³⁹ M. Lokajicek,¹¹ R. Lopes de Sa,⁷⁰ H. J. Lubatti,⁸⁰ R. Luna-Garcia,^{32,||} A. L. Lyon,⁴⁸ A. K. A. Maciel,² D. Mackin,⁷⁸ R. Madar,¹⁸ R. Magaña-Villalba,³² S. Malik,⁶⁴ V. L. Malyshev,³⁵ Y. Maravin,⁵⁷ J. Martínez-Ortega,³² R. McCarthy,⁷⁰ C. L. McGivern,⁵⁶ M. M. Meijer,³⁴ A. Melnitchouk,⁶³ D. Menezes,⁵⁰ P. G. Mercadante,⁴ M. Merkin,³⁷ A. Meyer,²¹ J. Meyer,²³ F. Miconi,¹⁹ N. K. Mondal,²⁹ G. S. Muanza,¹⁵ M. Mulhearn,⁷⁹ E. Nagy,¹⁵ M. Naimuddin,²⁸ M. Narain,⁷⁵ R. Nayyar,²⁸ H. A. Neal,⁶¹ J. P. Negret,⁸ P. Neustroev,³⁹ S. F. Novaes,⁵ T. Nunnemann,²⁵ G. Obrant,³⁹ J. Orduna,⁷⁸ N. Osman,¹⁵ J. Osta,⁵⁴ G. J. Otero y Garzón,¹ M. Padilla,⁴⁶ A. Pal,⁷⁶ N. Parashar,⁵³ V. Parihar,⁷⁵ S. K. Park,³¹ J. Parsons,⁶⁸ R. Partridge,^{75,‡} N. Parua,⁵² A. Patwa,⁷¹ B. Penning,⁴⁸ M. Perfilov,³⁷ K. Peters,⁴⁴ Y. Peters,⁴⁴ K. Petridis,⁴⁴ G. Petrillo,⁶⁹ P. Pétrouff,¹⁶ R. Piegaiia,¹ J. Piper,⁶² M.-A. Pleier,⁷¹ P. L. M. Podesta-Lerma,^{32,¶} V. M. Podstavkov,⁴⁸ P. Polozov,³⁶ A. V. Popov,³⁸ M. Prewitt,⁷⁸ D. Price,⁵² N. Prokopenko,³⁸ S. Protopopescu,⁷¹ J. Qian,⁶¹ A. Quadt,²³ B. Quinn,⁶³ M. S. Rangel,² K. Ranjan,²⁸ P. N. Ratoff,⁴² I. Razumov,³⁸ P. Renkel,⁷⁷ M. Rijssenbeek,⁷⁰ I. Ripp-Baudot,¹⁹ F. Rizatdinova,⁷⁴ M. Rominsky,⁴⁸ A. Ross,⁴² C. Royon,¹⁸ P. Rubinov,⁴⁸ R. Ruchti,⁵⁴ G. Safronov,³⁶ G. Sajot,¹⁴ P. Salcido,⁵⁰ A. Sánchez-Hernández,³² M. P. Sanders,²⁵ B. Sanghi,⁴⁸ A. S. Santos,⁵ G. Savage,⁴⁸ L. Sawyer,⁵⁸ T. Scanlon,⁴³ R. D. Schamberger,⁷⁰ Y. Scheglov,³⁹ H. Schellman,⁵¹ T. Schliephake,²⁶ S. Schlobohm,⁸⁰ C. Schwanenberger,⁴⁴ R. Schwienhorst,⁶² J. Sekaric,⁵⁶ H. Severini,⁷³ E. Shabalina,²³ V. Shary,¹⁸ A. A. Shchukin,³⁸ R. K. Shivpuri,²⁸ V. Simak,¹⁰ V. Sirotenko,⁴⁸ P. Skubic,⁷³ P. Slattery,⁶⁹ D. Smirnov,⁵⁴ K. J. Smith,⁶⁷ G. R. Snow,⁶⁴ J. Snow,⁷² S. Snyder,⁷¹ S. Söldner-Rembold,⁴⁴ L. Sonnenschein,²¹ K. Soustruznik,⁹ J. Stark,¹⁴ V. Stolin,³⁶ D. A. Stoyanova,³⁸ M. Strauss,⁷³ D. Strom,⁴⁹ L. Stutte,⁴⁸ L. Suter,⁴⁴ P. Svoisky,⁷³ M. Takahashi,⁴⁴ A. Tanasijczuk,¹ W. Taylor,⁶ M. Titov,¹⁸ V. V. Tokmenin,³⁵ Y.-T. Tsai,⁶⁹ D. Tsybychev,⁷⁰ B. Tuchming,¹⁸ C. Tully,⁶⁶ L. Uvarov,³⁹ S. Uvarov,³⁹ S. Uzunyan,⁵⁰ R. Van Kooten,⁵² W. M. van Leeuwen,³³ N. Varelas,⁴⁹ E. W. Varnes,⁴⁵ I. A. Vasilyev,³⁸

P. Verdier,²⁰ L. S. Vertogradov,³⁵ M. Verzocchi,⁴⁸ M. Vesterinen,⁴⁴ D. Vilanova,¹⁸ P. Vokac,¹⁰ H. D. Wahl,⁴⁷ M. H. L. S. Wang,⁶⁹ J. Warchol,⁵⁴ G. Watts,⁸⁰ M. Wayne,⁵⁴ M. Weber,^{48,**} L. Welty-Rieger,⁵¹ A. White,⁷⁶ D. Wicke,²⁶ M. R. J. Williams,⁴² G. W. Wilson,⁵⁶ M. Wobisch,⁵⁸ D. R. Wood,⁶⁰ T. R. Wyatt,⁴⁴ Y. Xie,⁴⁸ C. Xu,⁶¹ S. Yacoub,⁵¹ R. Yamada,⁴⁸ W.-C. Yang,⁴⁴ T. Yasuda,⁴⁸ Y. A. Yatsunenko,³⁵ Z. Ye,⁴⁸ H. Yin,⁴⁸ K. Yip,⁷¹ S. W. Youn,⁴⁸ J. Yu,⁷⁶ S. Zelitch,⁷⁹ T. Zhao,⁸⁰ B. Zhou,⁶¹ J. Zhu,⁶¹ M. Zielinski,⁶⁹ D. Zieminska,⁵² and L. Zivkovic⁷⁵

(D0 Collaboration)

- ¹Universidad de Buenos Aires, Buenos Aires, Argentina
²LAFEX, Centro Brasileiro de Pesquisas Físicas, Rio de Janeiro, Brazil
³Universidade do Estado do Rio de Janeiro, Rio de Janeiro, Brazil
⁴Universidade Federal do ABC, Santo André, Brazil
⁵Instituto de Física Teórica, Universidade Estadual Paulista, São Paulo, Brazil
⁶Simon Fraser University, Vancouver, British Columbia, and York University, Toronto, Ontario, Canada
⁷University of Science and Technology of China, Hefei, People's Republic of China
⁸Universidad de los Andes, Bogotá, Colombia
⁹Charles University, Faculty of Mathematics and Physics, Center for Particle Physics, Prague, Czech Republic
¹⁰Czech Technical University in Prague, Prague, Czech Republic
¹¹Center for Particle Physics, Institute of Physics, Academy of Sciences of the Czech Republic, Prague, Czech Republic
¹²Universidad San Francisco de Quito, Quito, Ecuador
¹³LPC, Université Blaise Pascal, CNRS/IN2P3, Clermont, France
¹⁴LPSC, Université Joseph Fourier Grenoble 1, CNRS/IN2P3, Institut National Polytechnique de Grenoble, Grenoble, France
¹⁵CPPM, Aix-Marseille Université, CNRS/IN2P3, Marseille, France
¹⁶LAL, Université Paris-Sud, CNRS/IN2P3, Orsay, France
¹⁷LPNHE, Universités Paris VI and VII, CNRS/IN2P3, Paris, France
¹⁸CEA, Irfu, SPP, Saclay, France
¹⁹IPHC, Université de Strasbourg, CNRS/IN2P3, Strasbourg, France
²⁰IPNL, Université Lyon 1, CNRS/IN2P3, Villeurbanne, France and Université de Lyon, Lyon, France
²¹III. Physikalisches Institut A, RWTH Aachen University, Aachen, Germany
²²Physikalisches Institut, Universität Freiburg, Freiburg, Germany
²³II. Physikalisches Institut, Georg-August-Universität Göttingen, Göttingen, Germany
²⁴Institut für Physik, Universität Mainz, Mainz, Germany
²⁵Ludwig-Maximilians-Universität München, München, Germany
²⁶Fachbereich Physik, Bergische Universität Wuppertal, Wuppertal, Germany
²⁷Panjab University, Chandigarh, India
²⁸Delhi University, Delhi, India
²⁹Tata Institute of Fundamental Research, Mumbai, India
³⁰University College Dublin, Dublin, Ireland
³¹Korea Detector Laboratory, Korea University, Seoul, Korea
³²CINVESTAV, Mexico City, Mexico
³³FOM-Institute NIKHEF and University of Amsterdam/NIKHEF, Amsterdam, The Netherlands
³⁴Radboud University Nijmegen/NIKHEF, Nijmegen, The Netherlands
³⁵Joint Institute for Nuclear Research, Dubna, Russia
³⁶Institute for Theoretical and Experimental Physics, Moscow, Russia
³⁷Moscow State University, Moscow, Russia
³⁸Institute for High Energy Physics, Protvino, Russia
³⁹Petersburg Nuclear Physics Institute, St. Petersburg, Russia
⁴⁰Institució Catalana de Recerca i Estudis Avançats (ICREA) and Institut de Física d'Altes Energies (IFAE), Barcelona, Spain
⁴¹Stockholm University, Stockholm and Uppsala University, Uppsala, Sweden
⁴²Lancaster University, Lancaster LA1 4YB, United Kingdom
⁴³Imperial College London, London SW7 2AZ, United Kingdom
⁴⁴The University of Manchester, Manchester M13 9PL, United Kingdom
⁴⁵University of Arizona, Tucson, Arizona 85721, USA
⁴⁶University of California Riverside, Riverside, California 92521, USA
⁴⁷Florida State University, Tallahassee, Florida 32306, USA
⁴⁸Fermi National Accelerator Laboratory, Batavia, Illinois 60510, USA
⁴⁹University of Illinois at Chicago, Chicago, Illinois 60607, USA
⁵⁰Northern Illinois University, DeKalb, Illinois 60115, USA
⁵¹Northwestern University, Evanston, Illinois 60208, USA

- ⁵²Indiana University, Bloomington, Indiana 47405, USA
⁵³Purdue University Calumet, Hammond, Indiana 46323, USA
⁵⁴University of Notre Dame, Notre Dame, Indiana 46556, USA
⁵⁵Iowa State University, Ames, Iowa 50011, USA
⁵⁶University of Kansas, Lawrence, Kansas 66045, USA
⁵⁷Kansas State University, Manhattan, Kansas 66506, USA
⁵⁸Louisiana Tech University, Ruston, Louisiana 71272, USA
⁵⁹Boston University, Boston, Massachusetts 02215, USA
⁶⁰Northeastern University, Boston, Massachusetts 02115, USA
⁶¹University of Michigan, Ann Arbor, Michigan 48109, USA
⁶²Michigan State University, East Lansing, Michigan 48824, USA
⁶³University of Mississippi, University, Mississippi 38677, USA
⁶⁴University of Nebraska, Lincoln, Nebraska 68588, USA
⁶⁵Rutgers University, Piscataway, New Jersey 08855, USA
⁶⁶Princeton University, Princeton, New Jersey 08544, USA
⁶⁷State University of New York, Buffalo, New York 14260, USA
⁶⁸Columbia University, New York, New York 10027, USA
⁶⁹University of Rochester, Rochester, New York 14627, USA
⁷⁰State University of New York, Stony Brook, New York 11794, USA
⁷¹Brookhaven National Laboratory, Upton, New York 11973, USA
⁷²Langston University, Langston, Oklahoma 73050, USA
⁷³University of Oklahoma, Norman, Oklahoma 73019, USA
⁷⁴Oklahoma State University, Stillwater, Oklahoma 74078, USA
⁷⁵Brown University, Providence, Rhode Island 02912, USA
⁷⁶University of Texas, Arlington, Texas 76019, USA
⁷⁷Southern Methodist University, Dallas, Texas 75275, USA
⁷⁸Rice University, Houston, Texas 77005, USA
⁷⁹University of Virginia, Charlottesville, Virginia 22901, USA
⁸⁰University of Washington, Seattle, Washington 98195, USA
(Received 28 April 2011; published 19 August 2011)

We measure the top quark mass (m_t) in $p\bar{p}$ collisions at a center of mass energy $\sqrt{s} = 1.96$ TeV using dilepton $t\bar{t} \rightarrow W^+bW^-\bar{b} \rightarrow \ell^+\nu_\ell b\ell^-\bar{\nu}_\ell\bar{b}$ events, where ℓ denotes an electron, a muon, or a tau that decays leptonically. The data correspond to an integrated luminosity of 5.4 fb^{-1} collected with the D0 detector at the Fermilab Tevatron Collider. We obtain $m_t = 174.0 \pm 1.8(\text{stat}) \pm 2.4(\text{syst}) \text{ GeV}$, which is in agreement with the current world average $m_t = 173.3 \pm 1.1 \text{ GeV}$. This is currently the most precise measurement of m_t in the dilepton channel.

DOI: 10.1103/PhysRevLett.107.082004

PACS numbers: 14.65.Ha

The measurement of the properties of the top quark has been a major goal of the Fermilab Tevatron Collider experiments since its discovery in 1995 [1,2]. As the heaviest known elementary particle, the top quark may play a special role in the mechanism of electroweak symmetry breaking. A precise measurement of its mass (m_t) is of particular importance, since, combined with the measurement of the W boson mass, it provides an indirect constraint on the mass of the Higgs boson in the standard model (SM) and can also constrain possible extensions of the SM.

We present a new measurement of the top quark mass in the dilepton channel (ee , $e\mu$, $\mu\mu$) in $t\bar{t} \rightarrow W^+bW^-\bar{b} \rightarrow \ell^+\nu_\ell b\ell^-\bar{\nu}_\ell\bar{b}$ events, where ℓ denotes an electron, a muon, or a tau decaying leptonically, using the matrix element method. The first measurement of m_t based on this method was performed in the lepton + jets channel by the D0 experiment [3]. The CDF Collaboration has applied the

matrix element approach to determine m_t in the dilepton and all-hadronic final states [4,5], obtaining a mass precision of 4.0 GeV for dilepton events [4]. The measurement of m_t in the dilepton channel has also been carried out by using other techniques [6–11], reaching a precision of 3.7 GeV. We report a measurement based on data collected by the D0 detector, corresponding to 5.4 fb^{-1} of integrated luminosity from $p\bar{p}$ collisions at $\sqrt{s} = 1.96$ TeV.

The D0 detector has a central tracking system, consisting of a silicon microstrip tracker and a central fiber tracker, both located within a 1.9 T superconducting solenoidal magnet [12], with the design providing tracking and vertexing at pseudorapidities $|\eta| < 3$ [13]. The liquid-argon and uranium calorimeter has a central section covering pseudorapidities $|\eta|$ up to ≈ 1.1 and two end calorimeters that extend coverage to $|\eta| \approx 4.2$, with all three housed in separate cryostats [14]. A muon system outside the calorimeters covers $|\eta| < 2$ and consists of a

layer of tracking detectors and scintillation trigger counters in front of 1.8 T toroids, followed by two similar layers after the toroids [15].

Despite the small branching fraction of this final state and the presence of two neutrinos in each event, the measurement of m_t in the dilepton channel is interesting because the lower background and the smaller jet multiplicity relative to the lepton + jets channel result in a reduced sensitivity to the ambiguity from combining jets in the reconstruction of m_t . The dilepton measurement therefore complements the results from other final states. Moreover, significant differences in measured values of m_t in different $t\bar{t}$ decay channels can be indicative of the presence of physics beyond the SM [16].

As the SM predicts top quarks to decay almost 100% of the time into a W boson and a b quark, $t\bar{t}$ events are classified according to the decays of the W boson. In the dilepton channel, both W bosons decay leptonically: $W^+ \rightarrow \ell^+ \nu_\ell$ [17] with $\ell = e, \mu, \text{ or } \tau$. We analyze the events characterized by two leptons $ee, e\mu, \text{ or } \mu\mu$, with a large transverse momenta (p_T), large imbalance in transverse momentum from the undetected neutrinos (\not{p}_T), and two high- p_T jets from the b quarks. The $W^+ \rightarrow \tau^+ \nu_\tau$ decays contribute through secondary $\tau^+ \rightarrow \ell^+ \nu_\ell \bar{\nu}_\tau$ transitions. For the ee and $\mu\mu$ analysis, we consider events selected by a set of single-lepton triggers. For the $e\mu$ channel, we use a mixture of single and multilepton triggers and lepton + jet triggers. Dilepton $t\bar{t}$ events are required to have at least two oppositely charged, isolated leptons with $p_T > 15$ GeV and either $|\eta| < 1.1$ or $1.5 < |\eta| < 2.5$ for electrons and $|\eta| < 2$ for muons. If more than one lepton-pair combination is found in an event, only the pair with the largest sum in scalar p_T is used. Events must have at least two jets with $p_T > 20$ GeV and $|\eta| < 2.5$, well separated from the selected electrons. No explicit b -jet identification is required in this analysis. The main sources of background in the dilepton channel are Drell-Yan and Z boson production ($Z/\gamma^* \rightarrow \ell^+ \ell^-$), diboson production (WW, WZ, ZZ), and instrumental background that originates from limited detector resolution and lepton misidentification. In the ee channel, the discrimination between the $t\bar{t}$ signal and background improves by requiring a large significance of the measured \not{p}_T , which is defined through a likelihood discriminant constructed from the ratio of \not{p}_T to its uncertainty [18]. In the $\mu\mu$ channel, we require, in addition, $\not{p}_T > 40$ GeV. In the $e\mu$ channel, the requirement $H_T > 115$ GeV, where H_T is the scalar sum of the transverse momenta of the leading lepton and the two leading jets, rejects most of the contribution from $\tau^+ \rightarrow \ell^+ \nu_\ell \bar{\nu}_\tau$. The above selections minimize the expected statistical uncertainty on m_t . In total, we select 479 candidate events with 73, 266, and 140 events, respectively, in the $ee, e\mu, \text{ and } \mu\mu$ channels, of which about $13 \pm 5, 48 \pm 15, \text{ and } 56 \pm 15$ events, respectively, are expected to arise from the background.

The matrix element method is based on the probability for a given event to resemble a signal, which depends on the value of m_t , or a background, which is usually independent of m_t . Assuming that the different physics processes leading to the same final state do not interfere, the event probability can be written as the sum of probabilities from all possible contributions. In practice, because the matrix element method requires significant computing time, only the dominant background is taken into account, and the total event probability is given by

$$P_{\text{evt}} = f_{t\bar{t}} P_{t\bar{t}}(x; m_t) + (1 - f_{t\bar{t}}) P_{Z+2\text{jets}}(x), \quad (1)$$

where $f_{t\bar{t}}$ is the fraction of $t\bar{t}$ events, $P_{t\bar{t}}$ and $P_{Z+2\text{jets}}$ are the signal and background probability densities, respectively, m_t is the assumed top quark mass, and x reflects the observed kinematic variables, i.e., the four-momenta of the measured jets and leptons. In the $ee, \mu\mu, \text{ and } e\mu$ channels, $Z + 2\text{jets}$ events with $Z \rightarrow e^+ e^-, Z \rightarrow \mu^+ \mu^-, \text{ and } Z \rightarrow \tau^+ \tau^- \rightarrow e^+ \nu_e \mu^- \bar{\nu}_\mu$ are the dominant source of background. The second leading background, from misidentified leptons, is approximately a factor of 3 smaller. While neglecting the other background probabilities leads to some bias, the calibration procedure described below allows us to correct for these and other limitations of the model.

The leading-order (LO) matrix element for $q\bar{q} \rightarrow t\bar{t} \rightarrow W^+ b W^- \bar{b} \rightarrow \ell^+ \nu_\ell b \ell^- \bar{\nu}_\ell \bar{b}$ is used to compute the $t\bar{t}$ probability density. For each final state y of the six produced partons, the signal probability is given by

$$P_{t\bar{t}}(x; m_t) = \frac{1}{\sigma_{\text{obs}}(m_t)} \cdot \sum_{i=1}^8 \int dq_1 dq_2 f_{\text{PDF}}(q_1) f_{\text{PDF}}(q_2) \cdot \frac{(2\pi)^4 |M(y; m_t)|^2}{q_1 q_2 s} d\Phi_6 W(x, y) W(p_T^{\bar{t}}), \quad (2)$$

where q_1 and q_2 denote the momentum fractions of the incident quarks in the proton and antiproton, respectively, f_{PDF} are the parton distribution functions (PDF) for finding a parton of a given flavor and longitudinal momentum fraction in the proton or antiproton (in this analysis we use the CTEQ6L1 PDF [19]), s is the square of the energy in the $q\bar{q}$ rest frame, $M(y)$ is the leading-order matrix element [20], and $d\Phi_6$ is an element of the 6-body phase space. Detector resolution is taken into account through a transfer function $W(x, y)$ that describes the probability of the partonic final state y to be measured as x . The finite transverse momentum of the $t\bar{t}$ system is accounted for through an integration over its probability distribution, which is derived from parton-level simulated events using ALPGEN [21], employing PYTHIA [22] for parton showers and hadronization. As the angular resolution of the jets and leptons, as well as the electron energy resolution, are sufficiently well determined, there is no need to introduce resolution functions. By taking into account energy and momentum conservation, Eq. (2) can be reduced to an

integration over the energies associated with the b quarks, the lepton-neutrino invariant masses, the differences between neutrino transverse momenta, the transverse momentum of the $t\bar{t}$ system, and the radii of curvature (p_T^{-1}) of muons. The sum runs over both possible jet-parton assignments and over up to two real solutions for each neutrino energy [23]. The normalization factor σ_{obs} is the product of the LO cross section and the mean efficiency of the final selections. A transfer function $W(x, y)$ is used for each jet and each muon in the final state. The jet energy resolution is parametrized as the sum of two Gaussian functions, with parameters depending linearly on parton energies, while the resolution in muon p_T^{-1} is described by a single Gaussian function. All parameters in $W(x, y)$ are determined from Monte Carlo (MC) $t\bar{t}$ events, tuned to match the resolutions observed in the data.

To take account of all background processes and to provide a correct statistical sampling of possible spin, flavor, and color configurations, the background probability $P_{Z+2\text{jets}}$ is calculated by using VECBOS [24]. Since $Z \rightarrow \tau^+ \tau^-$ decay is not modeled in VECBOS, an additional transfer function in the $e\mu$ channel is used to describe the energy of the final state lepton relative to the initial τ lepton, derived from parton-level information [23]. The direction of the final state lepton is assumed to be close to that of the τ lepton, since only in such cases is the lepton from the τ decay sufficiently energetic to pass the p_T selection. For the $(Z \rightarrow \tau^+ \tau^- \rightarrow e^+ \nu_e \mu^- \bar{\nu}_\mu) + 2\text{jets}$ probability, the energy fractions for final state leptons are sampled according to this τ transfer function. The jet and charged-lepton directions are assumed to be well-measured, and each kinematic solution is weighted according to the p_T of the $Z + 2\text{jets}$ system. The integration of the probability for $Z + 2\text{jets}$ is performed over the energies of the two partons that lead to the jets. Both possible assignments of jets to quarks are considered.

To calculate the signal and background probability densities, a MC-based integration of Eq. (2) is performed, and m_t is changed in steps of 2.5 GeV over a range of 30 GeV. For each mass hypothesis, a likelihood function $L_{\text{tot}}(m_t, f_{t\bar{t}})$ is defined by the product of individual event probabilities P_{evt} , and the signal fraction $f_{t\bar{t}}$ is determined by minimizing $-\ln L_{\text{tot}}$. Finally, the most likely value of m_t and its uncertainty are extracted from a fit of $L_{\text{tot}}(m_t)$ to a Gaussian form near its maximum by using the value of $f_{t\bar{t}}$ found in the previous step.

To check for any bias caused by approximations of the method, such as the use of the LO matrix element for $P_{t\bar{t}}$ or from neglecting backgrounds other than $Z + 2\text{jets}$, the measurement is calibrated by using MC events generated with ALPGEN+PYTHIA. All events are processed through a full GEANT3 [25] detector simulation, followed by the same reconstruction and analysis chain as used for the data. Effects from additional $p\bar{p}$ interactions are simulated by overlaying the data from random $p\bar{p}$ crossings over the

MC events. Five $t\bar{t}$ MC samples are generated with input top quark masses of $m_t = 165, 170, 172.5, 175,$ and 180 GeV. Probabilities for the $t\bar{t}$ signal and for $Z/\gamma^* \rightarrow \ell^+ \ell^-$, diboson, and instrumental backgrounds are used to form randomly drawn pseudoexperiments. The total number of events in each pseudoexperiment is fixed to the number of events in the data for the combined dilepton channels. The signal and background fractions are fluctuated according to multinomial statistics around the fractions determined from the measured $t\bar{t}$ cross section in the separate channels [26]. The mean values of m_t measured in 1000 pseudoexperiments as a function of the input m_t are shown in Fig. 1(a). The deviation from the ideal response, where the extracted mass is equal to the input mass, is caused both by the presence of backgrounds without a corresponding matrix element in the event probability and by approximations in the calculation of the $Z + 2\text{jets}$ probabilities. For the case of background-free pseudoexperiments, no difference is observed. The width of the distribution of the pulls (“pull width”), defined as the mean deviation of m_t in single pseudoexperiments from the mean for all 1000 values at a given input m_t , in units of the measured uncertainty per pseudoexperiment, is shown in Fig. 1(b). The statistical uncertainty measured in the data is corrected for the deviation of the pull width from unity. The calibrated value of m_t from the fit to the data is shown in Fig. 2(a). Figure 2(b) compares the measured uncertainty for m_t with the distribution of expected uncertainties in pseudoexperiments at $m_t = 175$ GeV. The difference between the observed and median expected uncertainty is not statistically significant. We also note that, when we change the signal to background ratio within uncertainties, the expected uncertainty generally increases and agrees well with the observation.

Systematic uncertainties on the measurement of m_t can be divided into three categories. The first involves uncertainties from modeling of the detector, such as the uncertainty on the energy scale of light-quark jets and the

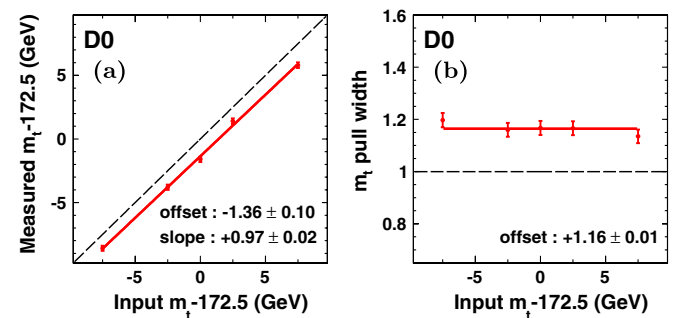


FIG. 1 (color online). (a) Mean values of m_t and (b) pull width from sets of 1000 pseudoexperiments as a function of input m_t for the combined dilepton channels. The dashed lines represent the ideal response in (a), where the extracted mass is identical to the input mass, and in (b), where the statistical uncertainty requires no correction.

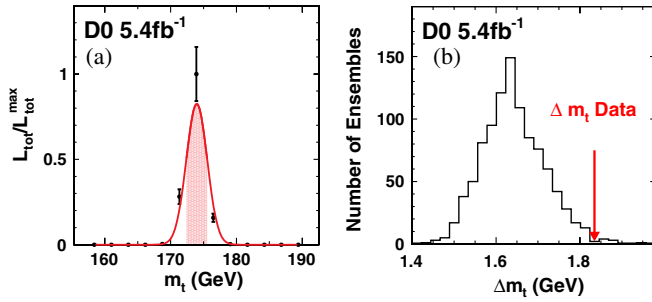


FIG. 2 (color online). Combined for all channels: (a) Calibrated and normalized likelihood for the data as a function of m_t with the best estimate as well as 68% confidence level region marked by the shaded area and in (b) the expected distribution of uncertainties with the measured uncertainty indicated by the arrow. As the top quark mass is measured to be $m_t = 174.0$ GeV, the expected distribution in (b) is shown for the closest input mass $m_t = 175$ GeV used in the pseudoexperiment.

uncertainty in the relative calorimeter response to b and light-quark jets, as well as in the energy resolution for jets, muons, and electrons. The second category is related to the modeling of $t\bar{t}$ production. This includes possible differences in the amount of initial and final state radiation, effects from next-to-leading-order contributions and different hadronization models, color reconnection, and modeling of b -quark fragmentation as well as uncertainties from the choice of PDF. The third category comprises effects from calibration, such as the uncertainties in the calibration function shown in Fig. 1(a), and from variations in signal and background contributions in the pseudoexperiments. Contributions to the total systematic uncertainty in the measurement of m_t are summarized in Table I.

The dominant systematic uncertainty arises from the different detector response of light and b -quark jets. It accounts for the different calorimeter response of single pions in the data and MC simulations and the different fractions of single pions in light and b -quark jets. The relative uncertainty of the response has been evaluated to be 1.8% leading to a shift of 1.6 GeV in m_t . The next important uncertainty comes from uncertainties in the jet energy scale (JES) of light quarks. This JES is calibrated by using γ + jets events [27]. More than 80% of the JES uncertainty is due to the understanding of the detector response and the showering of jets. The total uncertainty typically adds up to about 1.5% per jet, which translates into an uncertainty on m_t of 1.5 GeV. The main uncertainty from modeling $t\bar{t}$ production is from higher-order effects and hadronization. It is evaluated by using $t\bar{t}$ events generated with MC@NLO [28] and evolved in HERWIG [29]. The next leading uncertainty on modeling $t\bar{t}$ arises from the description of b -quark fragmentation. It is derived by comparing the extracted m_t for the default measurement with the result using a reweighting of the default MC samples to a Bowler scheme tuned to LEP or SLD data [30]. The largest difference is quoted as the uncertainty.

TABLE I. Summary of systematic uncertainties on the measurement of m_t in dilepton events.

Source	Uncertainty (GeV)
<i>Detector modeling:</i>	
b /light jet response	± 1.6
JES	± 1.5
Jet resolution	± 0.3
Muon resolution	± 0.2
Electron pT scale	± 0.4
Muon pT scale	± 0.2
ISR/FSR	± 0.2
<i>Signal modeling:</i>	
Higher order and hadronization	± 0.7
Color reconnection	± 0.1
b -quark modeling	± 0.4
PDF uncertainty	± 0.1
<i>Method:</i>	
MC calibration	± 0.1
Signal fraction	± 0.5
Total	± 2.4

In summary, we have presented a measurement of the top quark mass in the $t\bar{t} \rightarrow W^+ b W^- \bar{b} \rightarrow \ell^+ \nu_\ell b \ell^- \bar{\nu}_\ell \bar{b}$ channel using the matrix element method. Based on an integrated luminosity of 5.4 fb⁻¹ collected by the D0 Collaboration, the top quark mass is found to be

$$m_t = 174.0 \pm 1.8(\text{stat}) \pm 2.4(\text{syst}) \text{ GeV}. \quad (3)$$

This measurement is in good agreement with the current world average $m_t = 173.3 \pm 1.1$ GeV [31]. Its total uncertainty of 3.1 GeV corresponds to a 1.8% accuracy and represents the most precise measurement of m_t from dilepton $t\bar{t}$ final states.

We thank the staffs at Fermilab and collaborating institutions and acknowledge support from the DOE and NSF (USA); CEA and CNRS/IN2P3 (France); FASI, Rosatom, and RFBR (Russia); CNPq, FAPERJ, FAPESP, and FUNDUNESP (Brazil); DAE and DST (India); Colciencias (Colombia); CONACyT (Mexico); KRF and KOSEF (Korea); CONICET and UBACyT (Argentina); FOM (The Netherlands); STFC and the Royal Society (United Kingdom); MSMT and GACR (Czech Republic); CRC Program and NSERC (Canada); BMBF and DFG (Germany); SFI (Ireland); The Swedish Research Council (Sweden); and CAS and CNSF (China).

*Visitor from Augustana College, Sioux Falls, SD, USA.
[†]Visitor from The University of Liverpool, Liverpool, United Kingdom.
[‡]Visitor from SLAC, Menlo Park, CA, USA.
[§]Visitor from University College London, London, United Kingdom.

- ^{||}Visitor from Centro de Investigacion en Computacion-IPN, Mexico City, Mexico.
- [¶]Visitor from ECFM, Universidad Autonoma de Sinaloa, Culiacán, Mexico.
- ^{**}Visitor from Universität Bern, Bern, Switzerland.
- [1] F. Abe *et al.* (CDF Collaboration), *Phys. Rev. Lett.* **74**, 2626 (1995).
- [2] S. Abachi *et al.* (D0 Collaboration), *Phys. Rev. Lett.* **74**, 2632 (1995).
- [3] V.M. Abazov *et al.* (D0 Collaboration), *Nature (London)* **429**, 638 (2004).
- [4] A. Abulencia *et al.* (CDF Collaboration), *Phys. Rev. Lett.* **102**, 152001 (2009).
- [5] T. Aaltonen *et al.* (CDF Collaboration), *Phys. Rev. D* **79**, 072010 (2009).
- [6] T. Aaltonen *et al.* (CDF Collaboration), *Phys. Rev. Lett.* **100**, 062005 (2008).
- [7] T. Aaltonen *et al.* (CDF Collaboration), *Phys. Rev. D* **79**, 092005 (2009).
- [8] T. Aaltonen *et al.* (CDF Collaboration), *Phys. Rev. D* **79**, 072005 (2009).
- [9] T. Aaltonen *et al.* (CDF Collaboration), *Phys. Rev. D* **83**, 111101 (2011).
- [10] V.M. Abazov *et al.* (D0 Collaboration), *Phys. Lett. B* **655**, 7 (2007).
- [11] V.M. Abazov *et al.* (D0 Collaboration), *Phys. Rev. D* **80**, 092006 (2009).
- [12] V.M. Abazov *et al.* (D0 Collaboration), *Nucl. Instrum. Methods Phys. Res., Sect. A* **565**, 463 (2006).
- [13] The pseudorapidity η is defined relative to the center of the detector as $\eta = -\ln[\tan(\theta/2)]$, where θ is the polar angle with respect to the proton beam direction.
- [14] S. Abachi *et al.* (D0 Collaboration), *Nucl. Instrum. Methods Phys. Res., Sect. A* **338**, 185 (1994).
- [15] V.M. Abazov *et al.* (D0 Collaboration), *Nucl. Instrum. Methods Phys. Res., Sect. A* **552**, 372 (2005).
- [16] G.L. Kane and S. Mrenna, *Phys. Rev. Lett.* **77**, 3502 (1996).
- [17] Throughout this Letter, charge conjugated processes are included implicitly.
- [18] A.G. Schwartzman, Report No. FERMILAB-THESIS-2004-21.
- [19] J. Pumplin *et al.*, *J. High Energy Phys.* **07** (2002) 012.
- [20] G. Mahlon and S. Parke, *Phys. Lett. B* **411**, 173 (1997).
- [21] M.L. Mangano, M. Moretti, F. Piccinini, R. Pittau, and A.D. Polosa, *J. High Energy Phys.* **07** (2003) 001.
- [22] T. Sjöstrand, S. Mrenna, P. Skands, *J. High Energy Phys.* **05** (2006) 026.
- [23] F. Fiedler, A. Grohsjean, P. Haefner, and P. Schieferdecker, *Nucl. Instrum. Methods Phys. Res., Sect. A* **624**, 203 (2010).
- [24] F.A. Berends, H. Kuijf, B. Tausk, and W.T. Giele, *Nucl. Phys.* **B357**, 32 (1991).
- [25] R. Brun, F. Carminati, CERN Program Library Long Writeup Report No. W5013, 1993 (unpublished).
- [26] V.M. Abazov *et al.* (D0 Collaboration), *Phys. Lett. B* **702**, 16 (2011).
- [27] V.M. Abazov *et al.* (D0 Collaboration), *Phys. Rev. Lett.* **101**, 062001 (2008).
- [28] S. Frixione and B.R. Webber, [arXiv:hep-ph/0612272](https://arxiv.org/abs/hep-ph/0612272).
- [29] G. Corcella *et al.*, *J. High Energy Phys.* **01** (2001) 010.
- [30] ALEPH Collaboration, DELPHI Collaboration, L3 Collaboration, OPAL Collaboration, SLD Collaboration, LEP Electroweak Working Group, SLD electroweak, heavy-flavor groups, *Phys. Rep.* **427**, 257 (2006).
- [31] The Tevatron Electroweak Working Group (CDF and D0 Collaborations), [arXiv:1007.3178](https://arxiv.org/abs/1007.3178).